Peer-reviewed version available at *Aerospace* **2016**, *3*, 37; doi:10.3390/aerospace3040037

Article

Results of Long-Duration Simulation of Distant Retrograde Orbits

Gary Turner

Odyssey Space Research, 1120 NASA Pkwy, Houston, TX 77058, USA; gturner@odysseysr.com

Abstract: Distant Retrograde Orbits in the Earth-Moon system are gaining in popularity as stable 'parking' orbits for various conceptual missions. To investigate the stability of potential Distant Retrograde Orbits, simulations were executed, with propagation running over a thirty-year period. Initial conditions for the vehicle state were limited such that the position and velocity vectors were in the Earth-Moon orbital plane, with the velocity oriented such that it would produce retrograde motion about Moon. The resulting trajectories were investigated for stability against the eccentric relative orbits of Earth and Moon in an environment that also included gravitational perturbations from Sun, Jupiter, and Venus, and the effects of radiation pressure. The results appear to indicate that stability is enhanced at certain resonant states within the Earth-Moon system.

Keywords: Distant Retrograde Orbit; DRO; orbits–stability; radiation pressure; orbits–resonance; dynamics

1. Introduction

The term Distant Retrograde Orbit (DRO) was introduced by O'Campo and Rosborough [1] to describe a set of trajectories that appeared to orbit the Earth-Moon system in a retrograde sense when compared with the motion of the Earth/Moon around the solar-system barycenter. The same concept can be applied to any three-body problem; of particular interest are the trajectories of a vehicle in retrograde motion about Moon when viewed from the Earth-Moon barycenter.

The stability of the retrograde solution to the Hill problem (plane-restricted three-body problem where the mass of the second body is small) was earlier investigated by Hénon [2], with the conclusion that stable retrograde trajectories are theoretically possible at all radii in such a system. However, there are significant complications inherent in the real n-body problem representing a vehicle in the Earth-Moon system: a large and irregular second-body mass (Moon), eccentric orbits of the two primary bodies, out-of-plane perturbations from tertiary bodies, and radiation pressure from Sun are all unaccounted for in the simple analysis, and can all degrade the stability.

The theoretical long-duration stability feature of DROs has led to the recent consideration of DRO trajectories for several mission concepts, mostly in the Earth-Moon system. However, with its susceptibilty to those destabilizing forces described above, a lack of understanding of the long-term stability of such orbits adds significant and unnecessary risk to such mision concepts. The long-term effect on stability of these forces is not well catalogued, and there does not appear to be any comprehensive review of the stability of DROs in the Earth-Moon system.

Because most of these potential missions are in the Earth-Moon system, that is the most urgent system to consider. Thus, the analyses presented herein focus exclusively on retrograde orbits around Moon. The additional complexities of the real problem over the simple statement of Hill's problem complicates the analysis of the stability of DROs, with a meaningful analytical approach not available. Instead, a series of long-duration numerical simulations was processed.

Our simulations were conducted at the Johnson Space Center (JSC) using the JSC Engineering Orbital Dynamics (JEOD) environment and dynamics packages within the open-source Trick simulation engine. Numerical integration was performed with JEOD's implementation of the Livermore Solver for Ordinary Differential Equations (LSODE) integration algorithm, with Gauss-Jackson and Runge-Kutta (4th order) integrators used for generating verification data.

Planetary ephemerides were provided by JEOD's implementation of the DE421 Ephemeris model; this model provided the positions of the perturbing bodies discussed above.

In the first section, the nature of the problem and of the Distant Retrograde Orbit (DRO) is presented. Next, the non-Keplerian scenarios that can lead to elaborate resonant orbits are analyzed. This leads naturally into a discussion of initial conditions that lead to stable DROs. This work is further developed by adding radiation pressure as another perturbing force, and observing the consequential destabilizing effect. Finally, a more detailed analysis of the long-term evolution of orbital characteristics is performed, focusing on the family of stable DROs characterized by high lunar altitudes.

Nature of DROs

A major effect in the enhanced stability of retrograde trajectories over prograde trajectories is that retrograde trajectories can be produced with little or no gravitational influence from the secondary body, as discussed by Hénon [2] in the solution to the Hill problem. This is significant because minor bodies tend to be less homogeneous and therefore have gravitational fields that are less uniform. This lack of uniformity in the gravitational field is a major effect in the unstable nature of trajectories that are strongly gravitationally bound to minor bodies. While that strong gravitational bond is necessary for prograde trajectories about a secondary body, it is completely unnecessary for retrograde trajectories, especially those far from the body. Retrograde trajectories about a secondary body can be achieved by relying instead on the relative uniformity of the primary body's gravitational influence.

Consequently, The Distant Retrograde Orbits, operating at large distance from the secondary body are less influenced by the non-uniformity of the gravitational field, which enhances their stability. In this sense, the term "Distant" refers to orbits at distances beyond which orbits would normally be considered viable. The orbits are retrograde about the secondary body, opposite in the sense of the motion of the secondary body around the primary body.

To illustrate the concept of apparent orbital motion with negligible gravitational attraction, consider a vastly simplified scenario – the dance of two small vehicles under the influence only of a single gravitational body (e.g. two vehicles in low-earth-orbit). Both vehicles (A and B) are thus in standard Keplerian orbits about the single large body (the priamry body). Let us make these orbits have identical semi-major axis, with orbit A circular, and orbit B slightly eccentric. The two vehicles are placed in proximity to one another, such that when vehicle B is at periapsis, it is directly "below" vehicle A (i.e. on the radial line between the central gravitational body and vehicle A).

Because the two vehicles have the same semi-major axis, and vehicle B is at periapsis, vehicle B must be moving faster than vehicle A. It will advance ahead of A, even as it starts to move away from the central planet (e.g. Earth) to a higher altitude. Eventually, vehicle B will reach the same altitude as vehicle A, at which point it must be in front of vehicle A. As it continues to climb towards apoapsis, its orbital rate continues to decrease and vehicle A starts to gain on vehicle B again. As vehicle B reaches apoapsis, one half-orbit after starting, the two vehicles must again be on a radial line (they have identical orbital periods, so reach their half-orbit points simultaneously). The second half of the orbit proceeds as a mirror-image of the first, with vehicle B falling behind vehicle A as it descends, crosses the orbit of vehicle A behind it, and gains again to return to the starting point.

To an outside observer, vehicle B has just completed an orbit of vehicle A, and it has done so in a retrograde fashion (prograde being the direction of the orbit of both vehicles about the primary gravitational body). Equivalently, vehicle A appears to have completed a retrograde orbit about vehicle B. But the vehicles are small; there is no significant gravitational attraction between them, none is needed.

Thus, when considering retrograde orbits about some minor body in an n-body scenario, it is not necessary to restrict consideration to those orbits that are gravitationally bound to the minor body.

Conceptually, at least in a 3-body problem, orbits can go so far away from the minor body that its gravity becomes a minor contributor, even negligible when compared with that of the major body.

For the case of retrograde orbits about the moon, there are some additional limitations:

- The moon is sufficiently large and sufficiently close to Earth that it is not possible to position a vehicle in an orbit sufficiently far from Earth that it appears to orbit Moon without lunar gravity having a significant effect on the vehicle.
- The dominating influence of solar gravity makes the simplification to a 3-body problem solution unrealistic. The gravitational field is dominated by solar gravity, making the barycenter a non-inertial frame; this influence is time-dependent and out of the Earth-Moon plane that would otherwise define the Hill problem. At the very least, we have a 4-body problem.
- The perturbing effects of other celestial bodies, most notably Jupiter, impose additional time-dependent forces that further complicate the solution. These perturbations are also typically out of the Earth-Moon plane.

For this study, we will focus on the Earth-Moon system, with Earth being the primary body, Moon being the secondary body, with some arbitrary mass placed in retrograde orbit around Moon.

2. Results and Discussion

2.1. Stability of Resonant DROs

While Hénon [2] identified DROs as being generally stable, something causes a loss of long-term stability for DROs in the Earth-Moon system. The exact cause requires further investigation. However, it might be expected that the out-of-plane gravitational influences from Sun and Jupiter would be capable of degrading the stability. A focal point of this study is to investigate the effect of resonances within the Earth-Moon system as potential stabilizing factors against these out-of-plane perturbations.

The simulations conducted in this study tend to confirm this hypothesis; DROs with near-resonant states tend to be more stable than those in non-resonant states. However, the results serve to raise additional questions regarding the nature of the stable state-spaces. No theoretical analysis has been performed to justify or explain the simulation results; this paper focuses entirely on categorizing the numerical results from simulation.

2.1.1. Overview of Resonances

When considering the resonances, there are four values to consider in any given period of time:

- l, the number of times the vehicle moves around Earth in inertial space
- m, the number of times Moon moves around Earth in inertial space
- n, the number of times the vehicle moves around Moon in inertial space, and
- p, the number of times the vehicle moves around Moon in the Earth-Moon rotating frame.

Because the vehicle must stay in the proximity of Moon, $l \approx m$. Indeed, in the case of resonant states, the bodies must return to their original relative positions after one complete cycle (recognizing that one complete cycle could take several months), so equality is enforced over one complete cycle. Therefore, one of these values is redundant.

An additional simplification may be made to reduce the identification to two values. With n and p representing retrograde motion, geometry dictates that $p = m + n$. However, while any pair of these three values are therefore sufficient, the most appropriate choice of pair depends on the purpose for which it will be used. Therefore, we retain all three, and typically express them as *m:n:p* for the purpose of developing the concept.

Later in the document, when the discussion moves to stability of resonances, this gets abbreviated to a single value equal in value to $\frac{p}{m}$ with the recognition that all three values can then be

Peer-reviewed version available at Aerospace 2016, 3, 37; doi:10.3390/aerospace3040037

evaluated by arbitrarily selecting one. For example, a ratio of 2.5 evaluates to *2:3:5*, or could equally apply to *4:6:10*.

2.1.2. The Short Duration Resonances

The 1:0:1 Resonance

The simplest resonance is the one previously described, with a pair of vehicles in orbits of similar semi-major axes and slightly different eccentricities. In one orbit of Earth, the two vehicles appear to move around one another once when viewed in the rotating frame. However, when viewed in the inertial frame, that apparent motion completely changes form.

Consider Figure 1, illustrating the trajectories in inertial space over one orbit ($m = 1$). The Solid lines represent the orbital trajectories of two vehicles, with dashed lines showing the relative position of two vehicles, labeled x and y, during one complete orbit.

A The two vehicles are on the same radial line, with x at a higher altitude.
B y has advanced ahead of x and remains at lower altitude.
C y has advanced far ahead of x; the two are at comparable altitudes
D x begins the inevitable gain on y while descending to lower altitude.
E The two vehicles are again on the same radial line, but with x at the lower latitude.
F The two vehicles are again at comparable altitudes, with x now ahead of y.

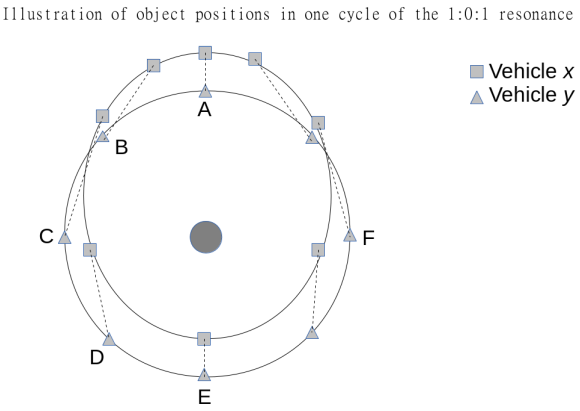

Figure 1. Schematic of the conceptual 1:0:1 resonance. The solid lines represent two different orbits. The dashed lines indicate the relative position of the two vehicles at snapshots in time.

It is apparent from Figure 1 that the vehicle x remains towards the top of the page relative to vehicle y throughout its motion. They never actually pass around one another in inertial space. Consequently, $n = 0$.

However, the relative altitude does shift. At position A, vehicle x has a greater altitude, and at position E, vehicle y has the greater altitude. Consequently, in the rotating frame, the two vehicles do appear to go around one another once. Hence, $p = 1$ (as expected, $p = m + n$).

Note that this works well for the case of light bodies where neither vehicle has a noticeable effect on the other and both follow Keplerian orbits. However, this is difficult to reproduce for our situation of interest because our vehicular trajectory, under the influence of two gravitational bodies, is non-Keplerian. For a vehicle in proximity to the moon with a semi-major axis comparable to that of the moon, it is simply unrealistic to assume that it will be largely unaffected by lunar gravity. No conditions were found that lead to a stable trajectory in this particular configuration.

Note also that for the case of light bodies orbiting a common central mass, both are constrained to move on Keplerian trajectories, and therefore this the only solution to provide retrograde trajectories around one another. Our case makes available significant additional forces (from Moon) that facilitate more complex resonances and highly-non-Keplerian trajectories.

The 1:1:2 Resonance

The *1:1:2* resonance looks somewhat similar to the *1:0:1* resonance, and is the most easily understood of the other resonances. In this pattern, the vehicle moves once around Moon as Moon moves once around Earth. In a rotating frame, the trajectory is such that it appears to make 2 passes around Moon while completing that one orbit.

Figure 2 illustrates snapshots of the trajectory for this resonance as observed in the Earth-centered inertial frame. Each snapshot of vehicle state is timestamped in sequence (t0 , t1 , t2 , t3). As the vehicle passes through this sequence, the relative position changes are described as follows:

1. The vehicle passes once around Earth in the inertial frame (above-left-below-right), moving counter-clockwise ($l = 1$).
2. The moon passes once around Earth in the inertial frame (above-left-below-right), moving counter-clockwise ($m = 1$).
3. The vehicle passes once around Moon in the inertial frame (below-left-above-right), moving clockwise ($n = 1$). Note that this is a retrograde motion.
4. The vehicle passes twice around Moon in the rotating frame (near-side – far-side – near-side – far-side, where "near-side" means the vehicle is between Earth and Moon, and "far-side" means the moon is between the vehicle and Earth). This motion is also clockwise, or retrograde. ($p = 2$).

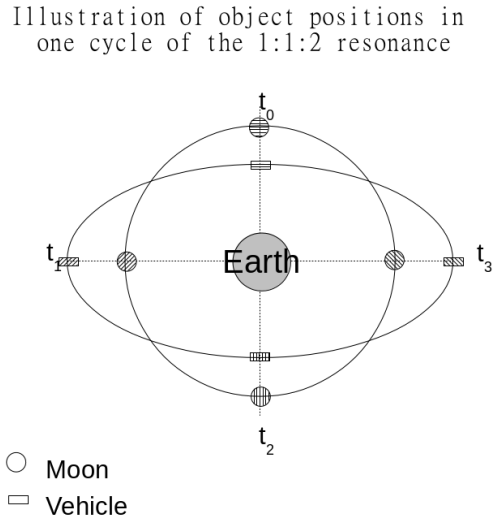

Figure 2. Illustration of the 1:1:2 resonance.

Notice that the vehicle orbit is quite definitely non-Keplerian. It is approximately elliptical, but with Earth at the center, not the focus, of the ellipse. This theoretical, geometrical solution is confirmed with simulation data. In Figure 3, the black line represents the lunar trajectory, and the red line the vehicular trajectory over a period of approximately 1 year. In this particular solution, the vehicular trajectory undergoes slow precession, the resonance is not perfect.

Preprints (www.preprints.org) | NOT PEER-REVIEWED | Posted: 1 August 2016 doi:10.20944/preprints201608.0002.v1

Peer-reviewed version available at Aerospace 2016, 3, 37; doi:10.3390/aerospace3040037

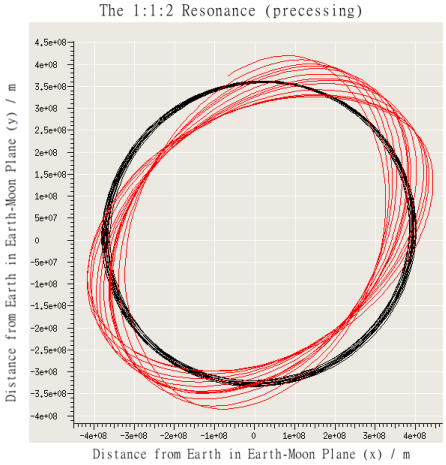

Figure 3. A slowly precessing 1:1:2 resonance. The black line (circular trajectory) represents the lunar orbit, and the red line (precessing oval trajectory) the DRO. Earth is at plot-center

The 1:2:3 Resonance

In one month, this resonance sees one prograde cycle of the vehicle relative to Earth, two retrograde cycles of the vehicle relative to Moon in the inertial frame, and three retrograde cycles of the vehicle relative to Moon in the rotating frame. Figure 4, again from simulation data, illustrates this pattern.

It is apparent now why we have retained the p term in the resonance identifier. The triangular trajectory in Figure 4 is more appropriately associated with the number 3 than with the number 2, even though it really is representing 2 Moon-cycles per Earth-cycle.

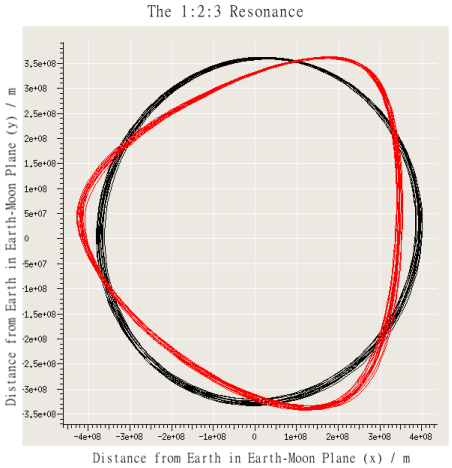

Figure 4. The 1:2:3 Resonance. The black line (circular trajectory) represents the lunar orbit, and the red line (triangular trajectory) the DRO.

The 1:x:x+1 Resonances

Higher order resonances are also easily found. A selection of these, the *1:3:4*, *1:5:6*, and *1:11:12* resonances, are shown in Figure 5.

The period for one earth orbit is fixed at one month; thus as the order increases, the period for one moon-orbit must decrease accordingly. Consequently, the higher order resonances have smaller vehicle-moon distances; thesee lower altitudes make the trajectories more susceptible to irregularities

Preprints (www.preprints.org) | NOT PEER-REVIEWED | Posted: 1 August 2016 doi:10.20944/preprints201608.0002.v1

Peer-reviewed version available at Aerospace 2016, 3, 37; doi:10.3390/aerospace3040037

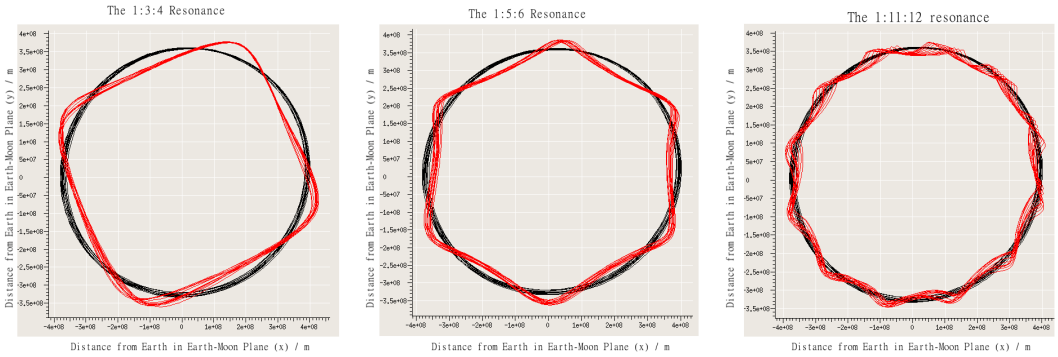

Figure 5. The *1:3:4*, *1:5:6*, and *1:11:12* Resonances. In each plot, the black line (circular trajectory) represents the lunar orbit, and the red line (non-circular trajectory) the DRO.

in the lunar gravity field and therefore less stable. Retrograde orbits close to the moon suffer from the same stability-destroying perturbations that were previously associated with prograde motion; the advantage of retrograde motion is lost in proximity to the moon, and these eventually become unstable at ratios of approximately 20. To find more DROs, it is necessary to keep the ratios low, thus requiring patterns on a multi-month timeframe, e.g. *2:3:5* = *2.5*, and *3:4:7* = *2.33*.

The 2:x:x+2 Resonances

Only those ratios comprising integers with no common denominator need to be considered, e.g., *2:1:3* and *2:3:5*. The *2:2:4* resonance is identical to the *1:1:2* resonance.

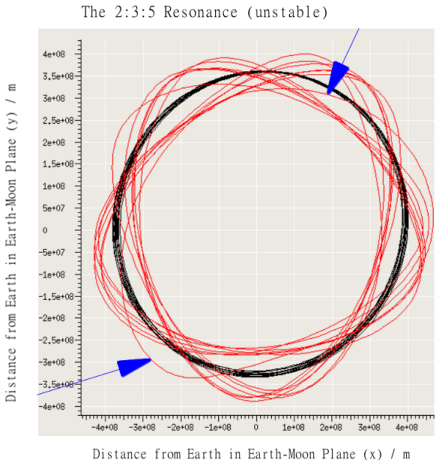

Figure 6. The *2:3:5* Resonance. The black line (circular trajectory) represents the lunar orbit, and the red line(irregular trajectory) the DRO. This trajectory was stable for only approximately 1 year; the final pass is identified with the blue arrows showing the divergence of the trajectory from its initially-settled path. The vehicle had a close lunar encounter and was ejected from the Earth-Moon system shortly after this data set was captured.

No resonance was identified with a *2:1:3* ratio; the analysis presented in section 2.2 confirms the complete absence of stable DROs at ratios below approximately 1.6. Additionally, while initial conditions were found for the *2:3:5* resonance, those conditions were not stable over a long period. Figure 6 represents the trajectory for a *2:3:5* resonance with data collected over approximately 1 year. The blue arrows identify the final pass before the stability collapses; it can be seen that the trajectory is starting to diverge from its cyclic pattern.

The 3:x:x+3 Resonances The *3:4:7* resonance was investigated and found to be stable over the long duration. With tri-monthly periods, the relative positions of the vehicle and Moon become difficult to visualize. Figure 7 shows the trajectory as in previous figures, and Figure 8 breaks that down into 16 steps, 4 steps per lunar orbit.

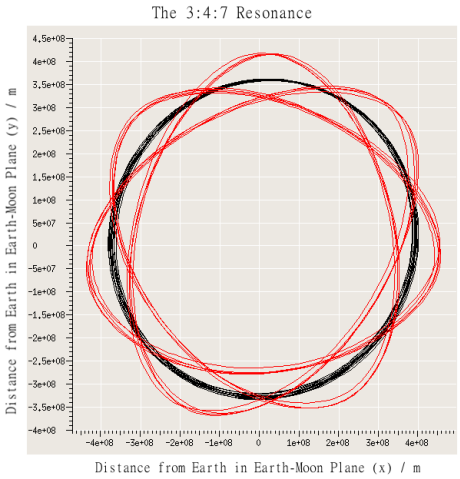

Figure 7. The *3:4:7* Resonance. The black line (circular trajectory)represents the lunar orbit, and the red line (7-pointed star) the DRO.

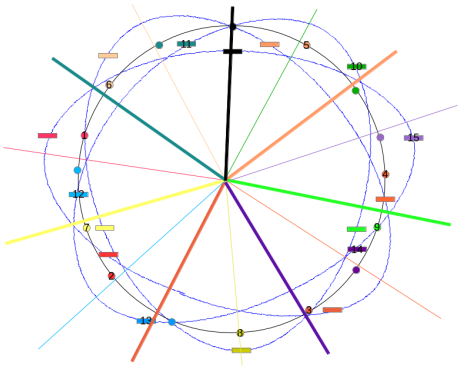

Figure 8. A timestamp breakdown of the 3:4:7 resonance in the Earth-centered inertial frame. Each timestamp includes a moon (small solid circle) and vehicle (rectangle). The moon and vehicle are color-matched, and each timestamp sequentially numbered. The grey circular line (on which the small circles are found) represents the trajectory of the moon, and the blue irregular line represents the trajectory of the vehicle. Starting at the top (black,0), both the moon and vehicle trace three earth-orbits before returning to the black state. The color-coordinated numerical sequence illustrates each quarter of the four lunar-orbits. The radial lines approximate the positions at which the vehicle is at inferior (thick lines) and superior (thin lines) locations relative to the moon; together, they illustrate the seven cycles in the rotating frame. The radial lines are color-coded to be close to the colors at a nearby time-stamp.

2.1.3. Longer Duration Resonances

Several long-duration stable ratios were identified, such as *6:5:11*, *6:7:13*, *7:8:15*, *6:11:17*, *3:8:11*, etc. However, distinguishing and defining these higher orders becomes challenging. For example, a 4:5:9 resonance effectively completes 2.25 rotating-frame cycles per month, a value that neatly bridges

Peer-reviewed version available at *Aerospace* **2016**, *3*, 37; doi:10.3390/aerospace3040037

the gap between 2 cycles of the 1:1:2 resonance and the 2.3 cycles of the 3:4:7 resonance. A state that is close to a perfect low-order resonance can easily be characterized as a slowly-precessing instance of that resonance. These states also tend to be stable.

Consequently, the distinction between a high-order long-duration resonance, such as 6:7:13, and a precessing low-order, short-duration resonance – such as 1:1:2 – is small. The characterization of such a trajectory one way over another becomes completely arbitrary. Thus, nothing was considered with a period longer than 8-months.

A selection of higher-order resonances is shown in Figure 9.

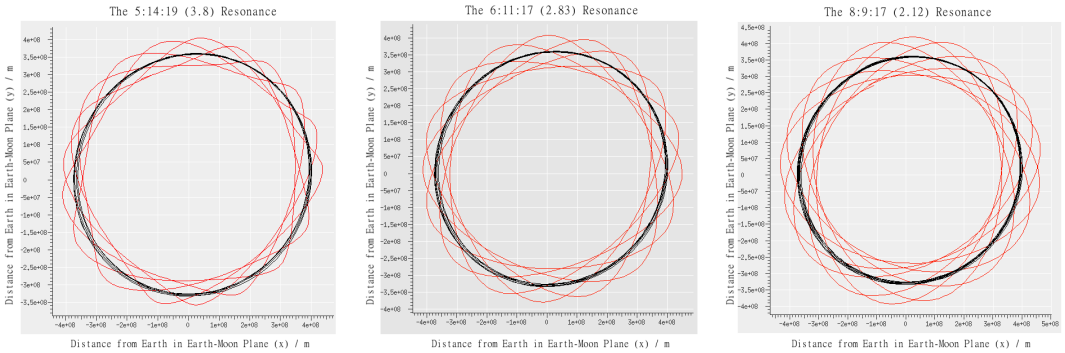

Figure 9. The *5:14:19* (*3.8*), *6:11:17* (*2.83*), *8:9:17* (*2.12*) resonances. In each plot, the black line (circular trajectory) represents the lunar orbit, and the red line (complex pattern) the DRO. Notice the peak altitudes increase as the ratio decreases.

2.2. Analysis of the Stability of DROs

To categorize the state space, the vehicle state is initialized with two parameters:

- distance from Moon, on the Moon-Earth position vector, and
- Moon-relative velocity in the Earth-Moon orbital plane, perpendicular to the Moon-Earth position vector.

Equivalently, consider a rectilinear local-vertical-local-horizontal (LVLH) reference frame with origin at Moon, referenced to Earth; in this frame, the initial vehicle state is characterized by

- the position, restricted to the LVLH-z-axis in the range $[1.7 \times 10^7, 1.2 \times 10^8]m$ (from Moon-center), and
- the velocity, restricted to the LVLH-x-axis in the range $[350, 600]ms^{-1}$.

Figures 10 - 11 illustrate which of these initial conditions produced trajectories that were stable for the 30-year duration of the simulation.

Each resonant DRO has a range of initial conditions, resulting in a resonant-specific characteristic curve in this state-space. As the initial distance between vehicle and Moon is increased, the initial speed must decrease in order to maintain the resonance. Thus, at any given initial position, each specific resonance will have a specific initial velocity, with the higher ratios (e.g. *1:11:12*) requiring a smaller speed than the lower ratios (e.g. *1:1:2*).

Similarly, at any specific initial velocity, there are a number of possible initial positions available, with the lower ratio resonances found at higher lunar-altitudes. Thus, in Figure 10, the characteristic curves for higher ratio resonances will be found towards the lower-left, with those for lower ratios towards the upper-right.

Figure 11 shows a large region of stability at relatively low lunar-altitudes with isolated islands of stability at higher lunar-altitudes. The stable regions in state-space tend to be associated with regions corresponding to resonances, but there are two very important observations here:

Preprints (www.preprints.org) | NOT PEER-REVIEWED | Posted: 1 August 2016 doi:10.20944/preprints201608.0002.v1

Peer-reviewed version available at Aerospace 2016, 3, 37; doi:10.3390/aerospace3040037

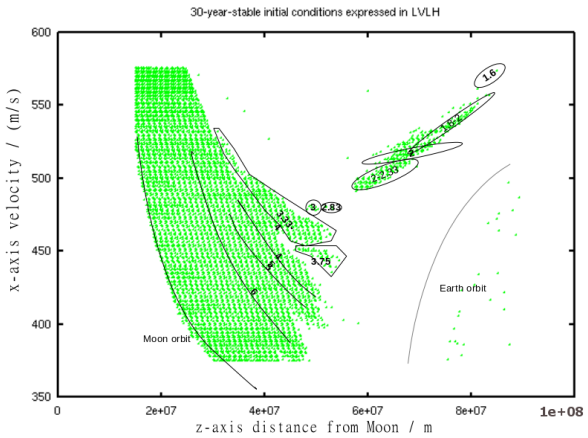

Figure 10. The initial states that remain stable over 30 years. The horizontal axis represents the initial position, measured along the LVLH z-axis; the vertical axis represents the initial velocity, directed along the LVLH x-axis. In the lower left, the states are sufficiently slow and close to the moon that they enter a lunar orbit. In the lower right, the vehicle never reaches the moon and enters an earth quasi-orbit. The numbers in the various regions indicate the approximate resonance ratios (e.g. *1:1:2 = 2; 4:11:15 = 3.75*), as determined by investigation of orbital characteristics in these regions.

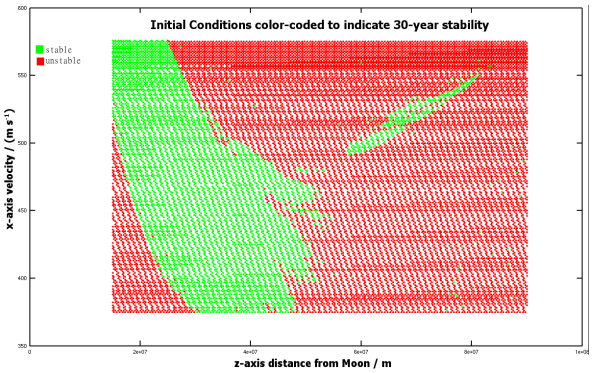

Figure 11. Superposition of the stable states from Figure 10 and the corresponding unstable initial states. Green (light shading) represents stable states, red (dark shading) represents unstable states. See also Figures 15 or 21 for more comprehensive data sets.

1. Not all resonances are present
2. Of those that are present, the stable zones surrounding those charactersitic curves are sized differently

Those resonances with the larger stable zones will tend to be the more useful for stationing a vehicle for a long period of time. They are going to be easier to hit, and more stable against perturbing influences which may easily shift the state out of a small stable zone. See the discussion on radiation pressure (section 2.4) for the significance of this consideration.

2.2.1. Analysis of Stable Zones

Notice from Figure 10 how the main region of stability covers ratios larger than 4. Between 3.33 and 4 there are two separate regions, separated by a small region of instability. The *1:2:3* ratio is stable over only a very small range. A large gap – representing an absence of stable states – extends from ratio 3 (*1:2:3*) to 2.33 (*3:4:7*), filled only by a couple of states in the *6:11:17* ratio which are of questionable stability. Of particular note, this means that there is no *2:3:5* (2.5) stable state.

Peer-reviewed version available at *Aerospace* **2016**, *3*, 37; doi:10.3390/aerospace3040037

In the lower corners of Figures 10-11, the vehicle goes into moon and earth orbits (left and right corners respectively) and fails to achieve the DRO trajectory. There are some stable hits in the earth-orbit area, but these are not DROs; see Figure 12 for a characteristic trajectory from this region. These trajectories are unlikely to be stable in the long term and may well prove to be unstable in the simulated environment if the state were integrated differently. However, their presence here does raise the possibility of their potential use as 'cycler-type' orbits requiring some limited degree of control authority to maintain stability.

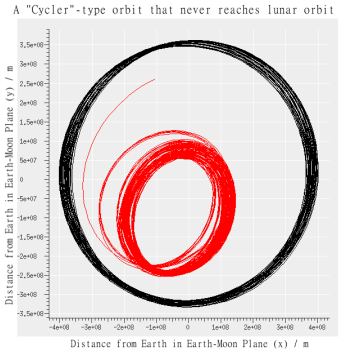

Figure 12. A characteristic trajectory in earth-inertial for a state taken from the lower right corner of the stability plot. The axes represent positions in the earth-centered reference frame. The black line (outer loop, circular trajectory) represents the moon's trajectory. The red line (inner loop) represents the vehicle trajectory. This is not representative of a DRO and its stability is highly questionable. There is potential for this type of orbit to be useful with the availability of some control authority.

Unstable trajectories are typically characterized as trajectories that have the vehicle coming close to the moon at some point and either crashing into it, or being ejected from the Earth-Moon system. In addition to the large islands of stable initial conditions, there are isolated initial states that generated stable states over the duration of the simulation; these are most likely associated with 'sweet spots' which result in ejection into a more stable orbit. They are not relevant to this study but the potential transition from an unstable region to a stable region deserves more study.

The left-hand edge of the main stable zone is questionably stable. Here, the vehicle is heavily influenced by lunar gravity and pulled into an elliptical and rapidly varying trajectory around the moon. Typically, the period and periapsis can vary significantly from one pass to another, see Figure 13 for an example.

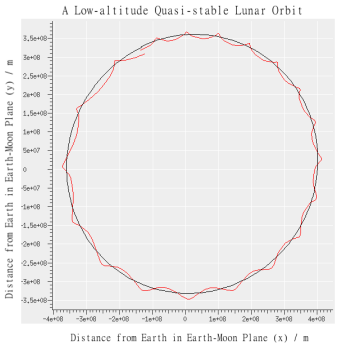

Figure 13. A characteristic trajectory over 1 month from the left-edge of the main stable zone in earth-centered coordinates. The black line (smooth circular shape) represents the trajectory of Moon. The red line (irregular pattern) represents the trajectory of a vehicle that was ultimately stable for 30 years.

During the first few simulated months, closer examination of the trajectories associated with initial conditions along this edge (as in Figure 13) demonstrates significant irregularities. While there are a few isolated instances where the trajectory becomes sufficiently unstable to eject the vehicle from the study, most of our simulated vehicles that have initial conditions in this region eventually stabilize and remain in the simulation for the full 30 years. This long-term stability resulting from short-term instability again suggests a transition process from unstable to stable conditions. Additional examples are discussed later with some preliminary data, but this is an area that deserves significantly more study.

2.3. Long-term Stability and Retention of Initial Conditions

2.3.1. Orbital Periods

Figure 13 illustrates a peculiar case in which the initial conditions produce a trajectory that appears to be quite unstable, but unexpectedly remains stable for the full 30-year simulation time. The presence of such conditions suggests that there may exist some mechanism to "attract" states from such a quasi-stable initial state-space into a more stable state-space. To further investigate this phenomenon, the evolution of stable trajectories is evaluated. The extent to which the state drifts away from the initial conditions is evaluated by testing for variations in the orbital periods of stable trajectories.

For this study, the orbital period is defined as the time interval between subsequent crossings of the LVLH y-z plane, with position at positive-z (between Earth and Moon).

The initial orbital periods for all initial conditions that resulted in at least one crossing of the y-z plane are shown in Figure 15. There are a couple of interesting points that can be immediately gleaned from this plot:

1. There are significant areas of the state-space for which no orbit is ever achieved (dark blue)
2. There are some very sharp transitions in the orbital period resulting from small adjustments to the initial position or velocity (e.g. $z = 5.4 \times 10^7\, m, v = 550\, ms^{-1}$, where the orbital period jumps by approximately a factor of 4)

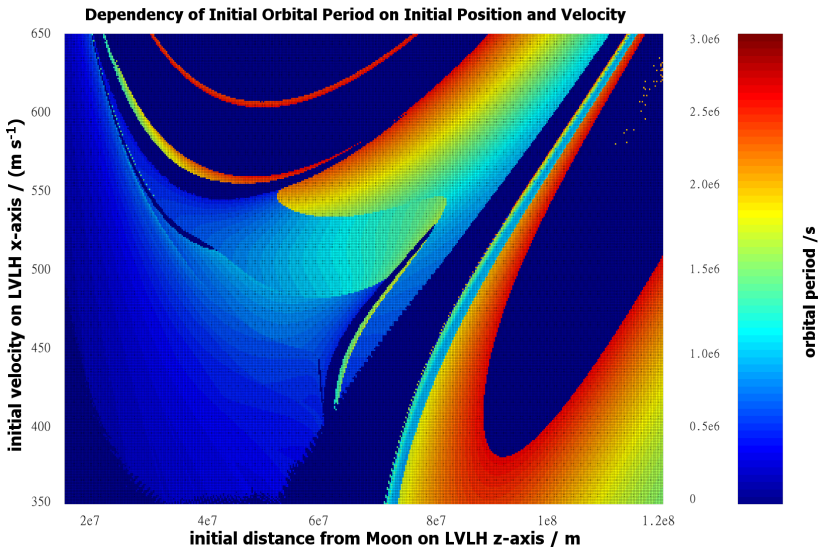

Figure 14. The initial orbital period in seconds (color-axis) as a function of the initial state. The horizontal axis represents the initial position (meters), measured along the LVLH z-axis; the vertical axis represents the initial velocity (m/s), directed along the LVLH x-axis. For reference, 1 sidereal month is approximately $2.4 \times 10^6\, s$

Peer-reviewed version available at Aerospace 2016, 3, 37; doi:10.3390/aerospace3040037

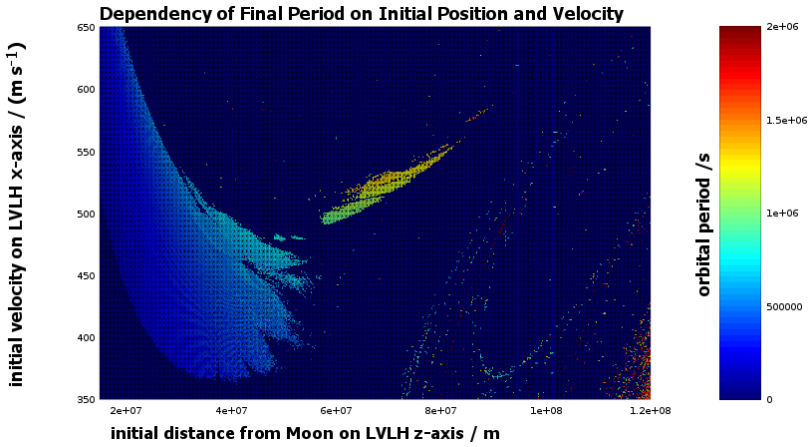

Figure 15. The final orbital period for those initial conditions that produced 30-year-stable trajectories. The axes are as described in Figure 14, and still represent the initial conditions. This plot can also be used to identify the 30-year-stable initial conditions. As such, it is similar to Figure 11, but provides more detailed coverage of the initial states.

The enhanced resolution in Figure 15 (over Figure 11) illustrates clean lines along the edges of some of the stable regions. This would suggest some theoretical limitation on the stability. Where these lines are replicated in Figure 14 (particularly the upper-right and lower-left of the main island), the limitation is very pronounced and should be identifiable from the simplified 3-body problem. This is another interesting area for further study.

2.3.2. Variation in Orbital Periods

If the initial states identified in Figure 15 were truly stable, then it would be expected that the initial periods and final periods (30 years later) would match. In many cases, the comparison is close, but there are exceptions. The differences between the initial and final periods are shown in Figure 16.

There are some interesting features in Figure 16, particularly noticeable in the latter plot:

1. In the stable island with $z \in [6,8] \times 10^7\, m$,the initial states on the lower right side tend to decrease in period, while the period of the states on the upper-left side tends to increase.
2. The pattern of stripes seen at the low-velocity end of the main island are not at all understood. They could be artifacts of the way the data was collected. This could be an interesting area for further study.
3. The noticeable reduction in period along the upper right of the main island corresponds to region of relatively high period in both the initial and final data sets (see Figures 14 - 15), and lies alongside a narrow strip of completely unstable initial conditions that failed to close a single orbit. (see Figure 14).

Another consideration is the standard deviation of the period of each vehicle throughout its 30-year data-set. This is shown in Figure 17. The completely stable initial states should show consistent periods and consequently low standard deviation. Points of interest from Figure 17 are listed below and identified more clearly in the higher resolution images presented in Figures 18 and 19. The causes of these features are not understood and warrant further investigation.

1. the deep blue region in the center of the $z \in [6,8] \times 10^7\, m$ island suggests that once established these orbits tend to be highly stable. Additionally, the initial conditions found in the upper-left area of this island show a significantly higher standard deviation than those states that lie in the lower-right area of this island. While it is expected that the initial conditions near the center line would be more stable, the asymmetry between the states "above" the center line and those

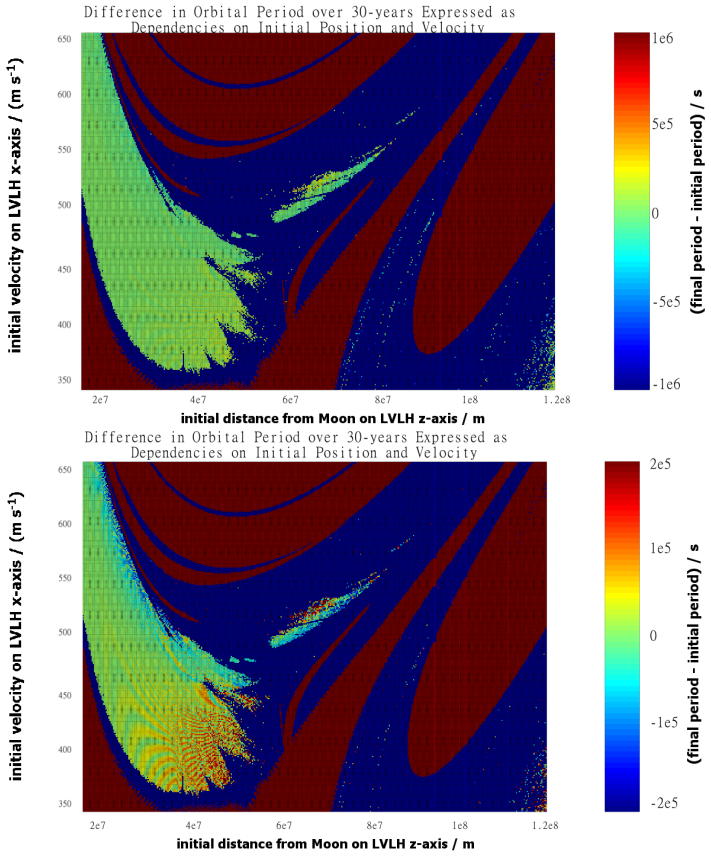

Figure 16. The difference in orbital periods between the data presented in Figures 14 and 15. The two plots show the same data sets, but differ in the choice of color-axis. The latter plot highlights those conditions that result in differences between inital and final period of less than two days. In both plots, the initial conditions that are not stable over 30 years are also shown. Those initial conditions that fail to produce a closed orbit are shaded dark red; those that complete the first orbit and subsequently become unstable are shaded dark blue.

"below" the line remains unexplained. This region is enhanced in Figure 18, and studied in more depth in section 2.5

2. the features in the main island. These are illustrated further in Figure 19.

A In the region $x \in [3.5 \times 10^7, 5.0 \times 10^7]\ m$, $y \in [460, 500]\ m\ s^{-1}$ there are two regions of low standard deviation and a narrow line of high standard deviation separating them.

B The lower left edge of the stable area described in A shows a sharp boundary (e.g. at $(3.8 \times 10^7\ m\ , 470\ m\ s^{-1})$. It appears almost as though there are two distinct dynamical processes, one in the background over a large range with a relatively large σ, and one with a smaller range and much lower σ that overrides the background process.

C A line of locally high standard deviation cuts through the background from $(2.5 \times 10^7\ m\ ,\ 550\ m\ s^{-1})$ to $(3.5 \times 10^7\ m,\ 450\ m\ s^{-1})$.

D A line of relatively low standard deviation around $(4.5 \times 10^7 m, 425 m s^{-1})$ to $(5.0 \times 10^7 m, 410 m s^{-1})$. The finger of stability surrounding this line appears to be associated with a particular resonance *(1:5:6)*. The low standard deviation on the line may be associated with the perfect resonance, and surrounded by states of near-resonance that are also stable.

2.4. Effect of Radiation Pressure

The effect of radiation pressure on the stability of a DRO is not possible to quantify in general terms because it depends on too many vehicle-specific parameters. The mass/volume ratio, the

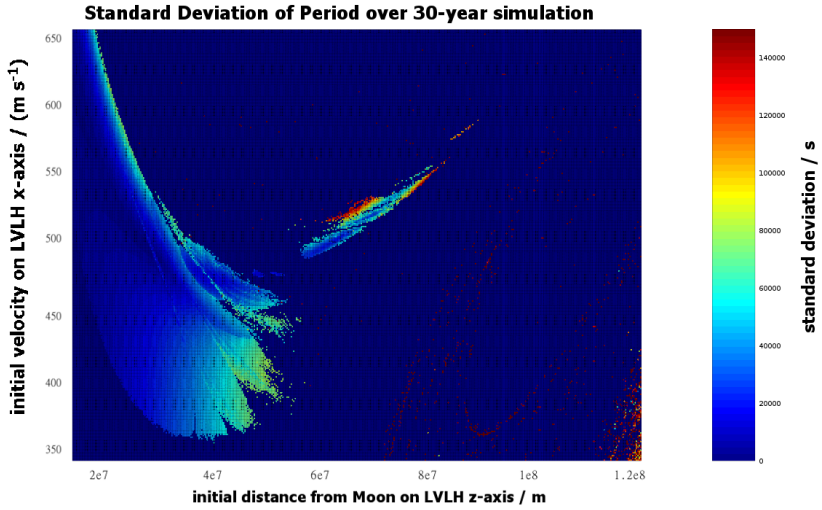

Figure 17. The standard deviation of the orbital period (color-axis) as a function of the initial state. As with Figures 14 - 16, the horizontal axis represents initial position (m) on the z-axis of the LVLH frame and the vertical axis represents the initial velocity ($m\,s^{-1}$) along the x-axis of the LVLH frame.

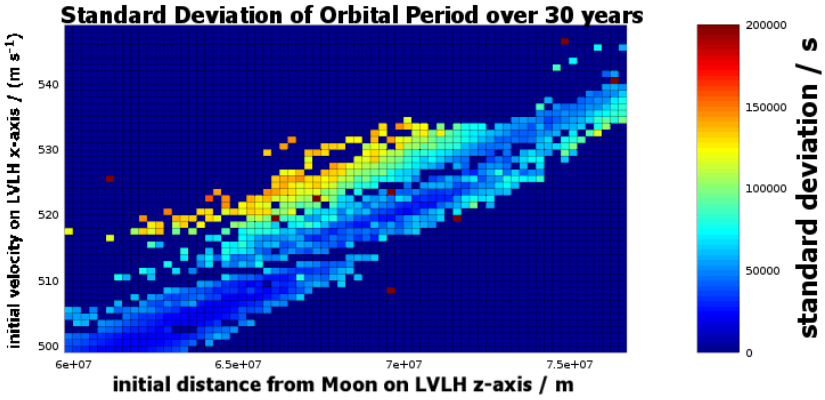

Figure 18. Replica of Figure 17 with higher resolution on the high-altitude region of interest.

geometry of the surface, the rotational state, the albedo and emissivity, and the nature of the reflection all affect the extent to which solar radiation pressure can affect the vehicle trajectory. Furthermore, particularly in the regions where the stability is marginal, the Yarkovsky effect (differential thermal emissions) can be significant over such long durations. This will be affected by rotation rate; heat capacities and distribution of surface materials; thermal conductivity within the vehicle; and location of thermal sinks and sources, such as solar panels or other power generators, and radiators.

Nevertheless, it is worth considering the potential for solar radiation pressure to affect the stability of the trajectories studied thus far. It is anticipated that the addition of another perturbing force will most likely destabilize those trajectories that were marginally stable (along the edges of the green areas in Figure 11) and have less effect on the more stable trajectories (deep within the green areas).

To test the effect, the vehicle was configured as a uniform isothermal sphere with perfect specular reflection. The simulations were terminated at five years (instead of thirty years) for reasons of simulation speed. Consequently, there will be some false positives, indicating that previously unstable states are now stable. However, the primary interest from this analysis is to identify which trajectories are destabilized by the presence of radiation pressure, not to identify isolated occurrences of apparent stabilization.

Peer-reviewed version available at Aerospace 2016, 3, 37; doi:10.3390/aerospace3040037

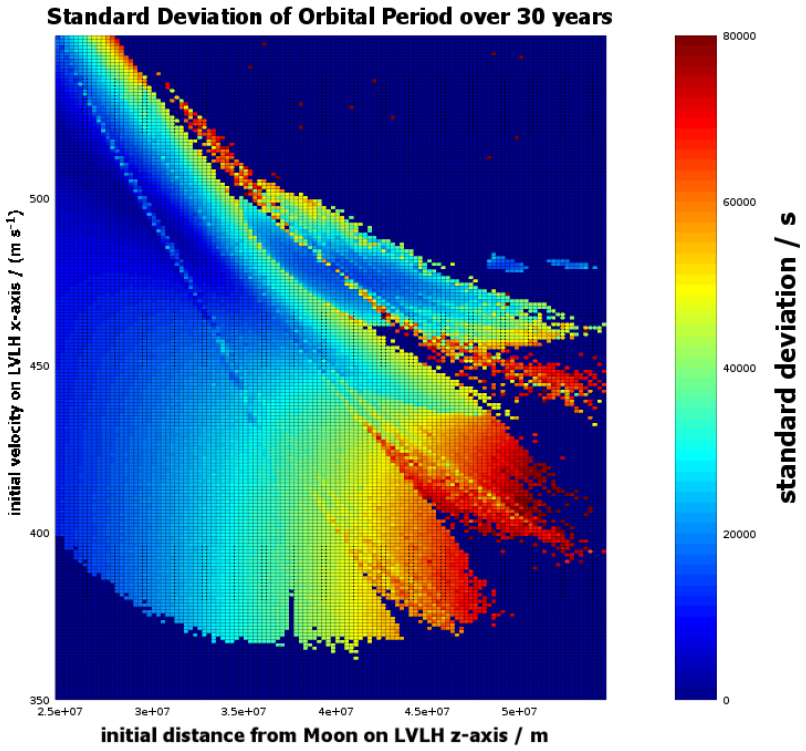

Figure 19. Replica of Figure 17 with regions of interest highlighted. Insert is an enhanced view of the region identified as A-C.

Three densities were tested:

- Very low density, $\rho = 10^{-3}\, kg\, m^{-3}$. This test was intended to confirm that radiation pressure perturbations would affect the stability of the trajectory.
- Low density, $\rho = 10^{0}\, kg\, m^{-3}$. This is still very low by spacecraft standards, but potentially relevant as a worst-case scenario for vehicles with large deployable arrays that would catch a significant pressure force without adding significantly to the mass. This effect is illustrated in Figure 20.
- Capsule-like density, $\rho = 10^{2}\, kg\, m^{-3}$. This is – to within an order of magnitude – comparable to a typical spacecraft capsule but still an order of magnitude below that of base materials. This effect is illustrated in Figure 21.

Very low density

Note – for reference, $10^{-3}\, kg\, m^{-3}$ is a comparable density to that of a large empty mylar envelope, or vaguely equivalent to a mylar sheet; it should be expected that radiation pressure would provide an enormous contribution to the net force. The test was by no means exhaustive, but no stable trajectories were found.

Low density

Figure 20 illustrates the overall effect of radiation pressure on the stability of a hypothetical low-density vehicle. The secondary islands of stability were effectively eliminated by this perturbation, leaving only the main region and a small region of stability around the *6:5:11* resonance. Of particular concern is the loss of almost all of the high-altitude stable region.

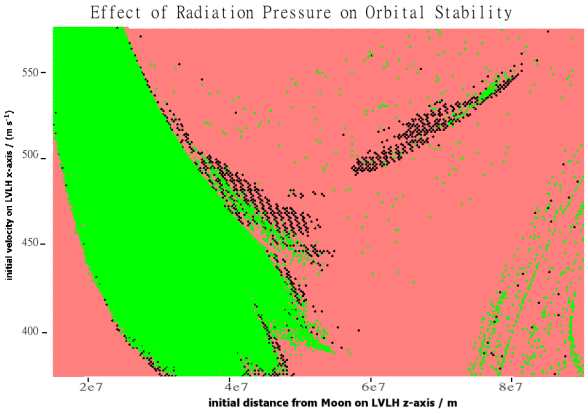

Figure 20. Superposition of the stable (green / light shading) and unstable (red / darker shading) states for the case with radiation pressure. States that were stable without radiation pressure and unstable with radiation pressure are identified with black dots. Most of the minor zones of stability have been destabilized by the effect of radiation pressure. Note – the black dots are taken from the limited data set used to generate Figures 10 - 11 and are set against a higher resolution data set. Consider the black dots as representative of area-shading rather than specific states.

The plethora of isolated stable states seen in Figure 20 that was not seen in Figure 11 is most likely a consequence of the reduced simulation time; it is reasonable to anticipate that many of these would not be stable over the full thirty years.

Capsule-like density

The results of the capsule-like density study are illustrated in Figure 21, using the full data set. With this density, radiation pressure had very little effect on the stability plots. The small 'islands' previously seen in Figure 10 at *1:2:3* (ratio =3) and at *6:11:17* (ratio = 2.83) are no longer stable, but the other regions are largely unaffected.

2.5. Detailed Study of the High-Altitude Stable Region

From Figure 21, five regions were identified in the high-altitude, $z \in [6,8] \times 10^7\, m$, region. Characteristic data points are taken from the center of each region. The data including radiation pressure was used to identify the candidate profiles, but the data itself was then extracted from the longer 30-year run without radiation pressure.

Table 1. Initial conditions for points in the center of stable islands

Initial position $/10^7\, m$	Initial velocity $/m\, s^{-1}$	Average period $/10^6\, s$	Period ratio	Possible resonance
6.00	498	1.028	2.3	3:4:7
6.45	507	1.105	2.13	7:8:15, 5:6:11?
6.95	519	1.191	2.0	1:1:2
7.075	529	1.274	1.85	6:5:11, 7:6;13?
7.725	539	1.271	1.86	6:5:11, 7:6;13?

Of these five, two are clearly associated with resonances, while three require the extension to higher orders, such as *7:6:13*, or *7:8:15*. Of interest is that the higher-order questionable resonances are symmetric about 2.0. Whether that is coincidental or a genuine feature of the dynamics is undetermined. But undeniably, the region with a period ratio of 2 is divided from the other stable conditions by instability bands; the reason why a period ratio of 1.86 ($T = 1.27 \times 10^7\, s$) is stable when

Preprints (www.preprints.org) | NOT PEER-REVIEWED | Posted: 1 August 2016 doi:10.20944/preprints201608.0002.v1

Peer-reviewed version available at Aerospace 2016, 3, 37; doi:10.3390/aerospace3040037

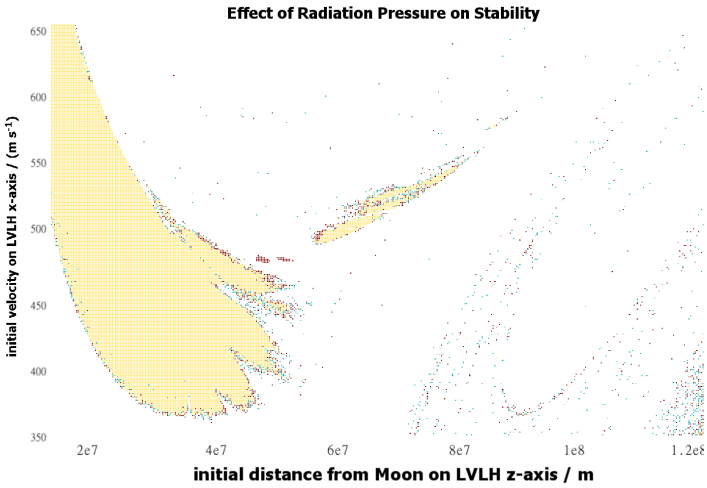

Figure 21. Graphical representation of the effect of radiation pressure on the stability of DROs. The horizontal axis represents the initial position (m), measured along the LVLH z-axis; the vertical axis represents the initial velocity ($m\,s^{-1}$), directed along the LVLH x-axis. The color axis is interpreted as: *Yellow / light shading – initial conditions that produce 30-year-stable trajectories without radiation pressure and 5-year-stable trajectories with radiation pressure. *Blue / medium shading – initial conditions that produce 5-year-stable trajectories with radiation pressure but did not produce 30-year-stable trajectories in the non-radiation pressure data set. *Red / dark shading – initial conditions that produce 30-year-stable trajectories without radiation pressure but fail to do so with radiation pressure.

1.95 ($T = 1.22 \times 10^7\ s$) is not, and why 2.13 ($T = 1.11 \times 10^7\ s$) is stable when 2.05 ($T = 1.15 \times 10^7\ s$) is not should be investigated further.

An additional effect appears when comparing the initial and final orbital period for each of the stable initial conditions. The variation with initial conditions of the initial orbital period is presented in Figure 22, while Figure 23 presents the variation with initial conditions of the final orbital period, some 30 years later. Both figures cover the same set of initial conditions, centered around the *1:1:2* resonance discussed in the previous paragraph. The dark blue regions represent those initial conditions that produce unstable trajectories.

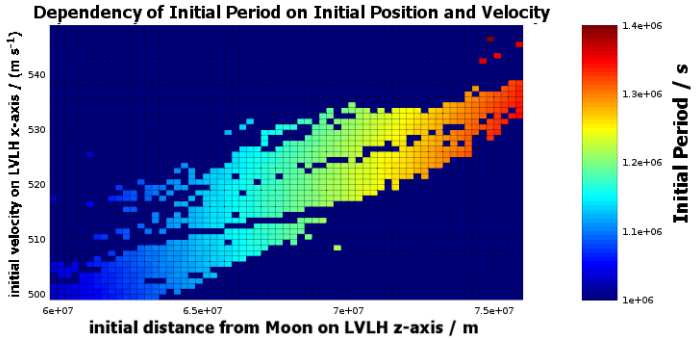

Figure 22. Detailed view of the initial orbital period, with the color axis in seconds. The data is restricted to those states for which the trajectory will be stable for 30 years.

Apparent from Figure 22, the initial period (color-axis) shows a strong dependency on the initial altitude (horizontal axis), and only a weak dependency on the initial velocity (vertical axis). The initial period varies continuously across the entire data set.

Peer-reviewed version available at Aerospace 2016, 3, 37; doi:10.3390/aerospace3040037

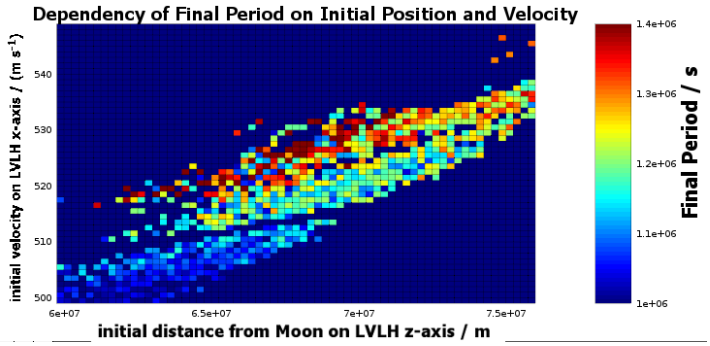

Figure 23. Detailed view of the final orbital period for the same initial conditions as Figure 22. The color-axis shows the period in seconds.

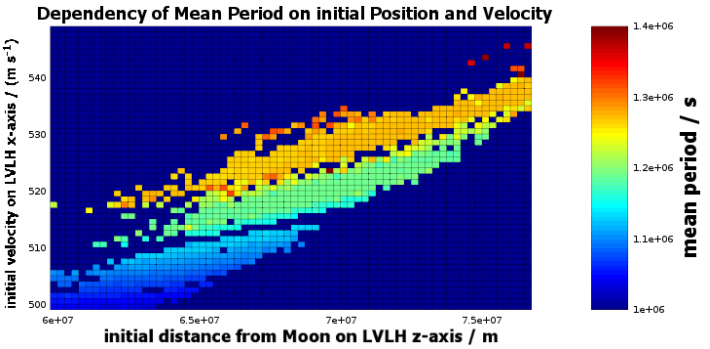

Figure 24. Detailed view of the mean orbital period for the same initial conditions as Figure 22. The color-axis shows the period in seconds.

The values of the final period are very much more chaotic than the values for the initial period; this is somewhat expected given the high standard deviation for parts of this region (illustrated in Figure 18). Whereas the initial period showed a strong dependency on initial altitude, the final period appears to have more dependency on the initial velocity.

This change in dominant dependency is more noticeable when considering the mean orbital period, as shown in Figure 24. In addition to the dependency change, the mean period values are also very much more discrete than the initial period values. Initial states comprising the upper island (ratios of approximately 1.85) result in a near-uniform mean-period. Initial states comprising the center island (period ratios of approximately 2.0) result in another near-uniform mean-period, distinct from the upper island. Finally, initial states comprising the lower island (ratios of > 2.0) result in a distribution of periods, but that distribution is still markedly different in nature than is the distribution of initial periods.

The process by which the trajectories transition from those that produce the initial periods to those at the end of the run is not understood and needs further investigation.

3. Conclusions

In general, it is not safe to assume that the DRO trajectory in the Earth-Moon environment is stable. There are some DROs that show long-term stability (i.e. stable over the entire 30-year simulation), and there is a strong correlation between the regions of position-velocity state space that produce stable DROs and the regions that produce resonant DROs. This suggests that the resonance may be directly linked to the stability of the DRO, but no causal effect has been identified.

Peer-reviewed version available at *Aerospace* **2016**, *3*, 37; doi:10.3390/aerospace3040037

3.1. Significance of Resonances

Some ratios have obviously resonant associations. For example, the integers and half-integers (e.g. 2.5, or *2:3:5*, conceptually completes five lunar orbits every two months) are clear. Less obvious are the more exotic values (e.g. 1.83 completes 11 lunar cycles in 6 months – i.e., *6:5:11*). Then there are the stable states that provide off-resonances, such as a 2.05 ratio. This could arguably be interpreted as a *20:21:41* resonant state (41 cycles in 20 months), or a forward-precessing *1:1:2* resonant state (2-and-a-bit cycles per month), or a non-resonant state.

There are certainly stable DROs with these off-resonant characteristics, and the choice of how to label these is entirely arbitrary. Nevertheless, when looking at the stability of all possible states, the data suggests that there are regions of stability that surround the simple low-integer resonant states. At the center of these regions are the perfect resonances, while farther from the center, the stability deteriorates as the states become off-resonant. Additionally, it is easy, statistically too easy, to find states that resonate strongly; this suggests that some of the perfectly resonant states may in fact be stable attractors to nearby off-resonant states, but much more work is needed in this area to confirm or disprove this hypothesis.

Conversely, there are some very basic resonances that have no identifiable stable region, and many that are stable only over a narrow region of state-space.

With the data currently available, the only conclusion that can be safely drawn is that there is a broad distribution of stable DROs; some of these are strongly associated with resonances in the Earth-Moon system, and some are not. Those that are not perfect resonances can usually be characterized as being close to a resonance (see Figure 3). Whether this characterization is helpful or has merit is left to the reader's discretion until further analysis can be performed.

3.2. Theoretical Analysis of Stability

No theoretical analysis of the stability has been performed, but the structure immediately apparent in the initial-period plot (Figure 14) would tend to suggest that there should be some analytical justification for immediate identification of initial conditions that would lead to unstable trajectories.

3.3. Addition of Perturbations

The addition of radiation pressure as another perturbing force further degrades the stability of the DROs. The significance of this result is two-fold:

1. It lends support to the hypothesis that other perturbing influences (such as third-body gravitational effects) may be responsible for the loss of stability in the general DRO trajectory.
2. It means that vehicle configuration is a significant consideration in determining the long-term stability of parking a vehicle in a DRO.

It should be noted that the radiation pressure model used for this analysis included direct-illumination only. While shadowing effects of Earth and Moon were included, albedo effects (i.e. pressure resulting from their reflected light) were not.

3.4. Evolution of Orbital Characteristics

There is some data – particularly along the edges of the stable zones and for stable trajectories with orbital ratios between 1.85 and 2.33 – that suggest the orbital characteristics evolve over time, from marginally-stable trajectories to something more stable. This could partially explain the clustering of initial states leading to 30-year stable trajectories. This paper considers only the long-term (i.e. 30-year) stability of initial states; no analysis has been performed to compare the characteristics of trajectories after allowing for those trajectories to evolve.

Acknowledgments: I would like to acknowledge Dr. Robert Shelton for recognizing the potential significance of this work, encouraging its publication, and for reviewing the document.

Conflicts of Interest: The author declares no conflict of interest.

References

1. O'Campo, C.A, ; Rosborough, G.W. Transfer trajectories for distant retrograde orbiters of the Earth. *NASA STI/Recon Technical Report A 95 1993: 81418* **1993** ISSN 0065-3438, pp1177-1200.
2. Hénon, M. Numerical exploration of the restricted problem. VI. Hill's case: Non-periodic orbits. *Astronomy and Astrophysics* **1970** *Vol 9*, pp24-36.